Journal of Hydrology 529 (2015) 1282–1292

Contents lists available at ScienceDirect

Journal of Hydrology

journal homepage: www.elsevier.com/locate/jhydrol

The effect of salinization and freshening events in coastal aquifers on nutrient characteristics as deduced from column experiments under aerobic and anaerobic conditions

A. Russak [a,b,*], O. Sivan [a], B. Herut [c], B. Lazar [d], Y. Yechieli [b,e]

[a] Department of Geological and Environmental Sciences, Ben Gurion University of the Negev, Beer Sheva, Israel
[b] Geological Survey of Israel, Jerusalem, Israel
[c] Israel Oceanographic and Limnological Research, National Institute of Oceanography, Haifa, Israel
[d] Institute of Earth Sciences, Hebrew University, Jerusalem, Israel
[e] Department of Environmental Hydrology & Microbiology, Zuckerberg Institute for Water Research, Blaustein Institute for Desert Studies, Ben Gurion University of the Negev, Sede Boqer, Israel

ARTICLE INFO

Article history:
Available online 30 July 2015

This manuscript was handled by Corrado Corradini, Editor-in-Chief, with the assistance of Christophe Darnault, Associate Editor

Keywords:
Coastal aquifer
Seawater intrusion
Fresh–saline groundwater interface
Column experiments
Nitrogen
Phosphate

SUMMARY

This study experimentally quantified the effect of seawater intrusion (salinization) and freshening events in coastal aquifers on nutrient (N, P and DSi) dynamics across the fresh–saline groundwater interface. Laboratory column experiments were conducted under aerobic and anaerobic conditions in order to simulate the processes occurring in the fresh–saline interface. They were performed with aquifer sediments, simulating the natural conditions during alterations of natural fresh groundwater to seawater and vice versa. The salinization and freshening experiments showed that NH_4^+ and PO_4^{3-} and DSi were affected mainly by ion exchange processes while microbial activity controlled the nitrogen species NO_3^- and NO_2^-. Due to the cation exchange, salinization generated enrichment (above the expected conservative behavior) of NH_4^+, up to 80 μmol L^{-1} (an order of magnitude higher than in seawater or fresh groundwater). Under anaerobic conditions NO_3^- was removed by denitrification, as demonstrated by the decrease in NO_3^- concentrations, the increase in NO_2^- concentrations, and the increase in $\delta^{15}N$ by 15–25‰. Clear evidence was shown for anion exchange of PO_4^{3-}, which competes with HCO_3^- and boron on adsorption sites. DSi seems to take part in the exchange process, similar to PO_4^{3-}.

1. Introduction

The current global intrusion of seawater into coastal aquifers causes salinization of groundwater, by replacing fresh groundwater with seawater and shifting the fresh–saline water interface (FSI) inland (e.g., Jones et al., 1999; Andersen et al., 2005). Column experiments can improve our understanding regarding how salinization and freshening events can influence the physical and geochemical characteristics of the FSI (e.g., Russak and Sivan, 2010). However, there are only a few studies of salinization and freshening in column experiments (e.g., Gomis-Yagues et al., 1997) and only one study included NH_4^+ and it was conducted entirely under anaerobic conditions (Appelo et al., 1990; Beekman and Appelo, 1991). The current study focuses on the nutrients' behavior when water in the column switches from freshwater to seawater and vice versa, under both aerobic and anaerobic conditions.

The FSI is potentially an active zone for nutrient transformations due to possible changes in salinity and dissolved oxygen (DO) levels. While fresh groundwater is usually aerobic, the saline groundwater may be anoxic to suboxic (Sivan et al., 2005). The oxic fresh groundwater may meet anoxic or suboxic saline groundwater in the FSI (Slomp and Van Cappellen, 2004). Santoro (2010) described the importance of the FSI to nitrogen cycling by microbial activities and referred to studies in environments with oxic fresh groundwater and anoxic saline groundwater (Tobias et al., 2001; Addy et al., 2005; Charette, 2007) or suboxic saline groundwater (Ullman et al., 2003; Charette et al., 2005).

Different dissolved oxygen (DO) levels can result in diverse biological processes. Ammonium (NH_4^+) may take part in nitrification, which is a multi-step oxidation process mediated by autotrophic organisms (e.g., Kendall, 1998; Santoro, 2010). The reaction

* Corresponding author at: P.O.B. 653, Beer Sheva 84105, Israel. Tel.: +972 8 6477506.
E-mail addresses: russak@bgu.ac.il (A. Russak), oritsi@bgu.ac.il (O. Sivan), barak@ocean.org.il (B. Herut), boaz.lazar@huji.ac.il (B. Lazar), yechieli@gsi.gov.il (Y. Yechieli).

http://dx.doi.org/10.1016/j.jhydrol.2015.07.034
0022-1694/

produces nitrate (NO_3^-) and intermediate species such as nitrite (NO_2^-). The NO_3^- may later be denitrified to N_2. Denitrification accounts for the main biological process which removes NO_3^-, performed by reducing gaseous N_2 (via NO_2^-) under suboxic to anoxic conditions (Bear, 1964; Santoro, 2010), when DO concentration is limited to less than 0.5 mg L^{-1} (Kendall, 1998). The denitrification rate decreases with increasing salinity (Rysgaard et al., 1999). There is another process that removes NO_3^- and reduces it to NH_4^+ called dissimilatory nitrate reduction to ammonium (DNRA). Recently, studies showed that DNRA can be an important pathway of nitrogen species (Giblin et al., 2013). It seems that in a system with a load of organic carbon and a high rate of sulfate reduction, DNRA may be favored over denitrification (Giblin et al., 2013). In addition, there is another biological process that removes nitrogen from the system, namely anaerobic ammonium oxidation (anammox). This process utilizes NH_4^+ and NO_2^- under anaerobic conditions to form N_2 (e.g., Dalsgaard et al., 2003). The contribution of anammox to nitrogen removal is higher in nutrient rich systems such as waste water, upwelling, marshes, etc. (Kuenen, 2008).

The DIN isotopic values can serve as indicators for sources and biological transformations in oxic and anoxic waters (e.g., Montoya and Voss, 2006). When combining $\delta^{15}N$ with $\delta^{18}O$, the isotopic analysis enables a more precise characterization of the sources and processes of nitrate and nitrite, rather than using ^{15}N alone (Kendall, 1998). During denitrification, the ^{15}N and ^{18}O of the residual NO_3^- are enriched (e.g., Mariotti et al., 1981, 1988; Kendall and Aravena, 2000). The fractionation factor for denitrification in the ocean was found to be 20–30‰ (e.g., Cline and Kaplan, 1975; Altabet et al., 1999; Voss et al., 2001). The expected ratio between $\delta^{18}O$ and $\delta^{15}N$ in denitrification and assimilation is 1:1 (e.g., Casciotti et al., 2002; Sigman et al., 2003). However, there are some deviations from this ratio in ocean samples. Nitrification can cause these variations since the nitrogen's source is the organic matter while the oxygen's source is the dissolved oxygen in the water and the water itself (Kendall, 1998).

The main process that is known to affect ammonium concentrations in the FSI is cation exchange. However, no previous study has compared the process of cation exchange conducted under aerobic conditions to that conducted under anaerobic conditions. NH_4^+ tends to be adsorbed on organic matter and clays, but not on calcium carbonate (Rosenfeld, 1979). It was shown that NH_4^+ is more readily adsorbed on particles in fresh water than in saline water (Seitzinger et al., 1991). Furthermore, increased salinity immediately releases NH_4^+ with corresponding intensities (Baldwin et al., 2006). Column laboratory experiments simulating salinization and freshening events under anaerobic conditions showed an NH_4^+ increase during salinization and a decrease during freshening due to cation exchange (Appelo et al., 1990; Beekman and Appelo, 1991).

Adsorption of phosphorus (P) on calcium carbonate sediments may affect phosphate (PO_4^{3-}) limitation in marine systems (De Kanel and Morse, 1978). The adsorption is reversible and the desorption process occurs even faster than the adsorption (Sø et al., 2011). Laboratory experiments showed that PO_4^{3-} adsorbed on calcium carbonate particles due to competition between HCO_3^- and PO_4^{3-} (Price et al., 2010). An increase in HCO_3^- concentration decreases the PO_4^{3-} adsorption, particularly when the salinity is low and the effect of HCO_3^- is greater than the effect of salinity (Millero et al., 2001). It seems that borate also competes with PO_4^{3-} for exchange sites (e.g., Mayer and Gloss, 1980; Goldberg, 1997). Phosphorus can also be adsorbed on Fe(III) and Mn(IV) hydroxides (e.g., Fonseca et al., 2011). Thus, oxidation of Fe^{2+} can result in PO_4^{3-} adsorption, while Fe(III) oxide reduction can result in PO_4^{3-} release (Spiteri et al., 2008). Phosphorus species are adsorbed differently on different Fe(III) hydroxides, but their isotherms and kinetics were shown to be similar (Ruttenberg and Sulak, 2011).

Dissolved silica (DSi) can be affected by salinization and freshening events. It was shown experimentally that the DSi concentration increased with salinity, as a result of the dissolution of biogenic silica (Yamada and D'Elia, 1984). Moreover, enrichment of DSi due to seawater intrusion was explained by the dissolution of biogenic opal (Stuyfzand, 1993). However, when biogenic silica does not exist in the system, clay minerals can control DSi concentration by sorption processes (Siever, 1992). Other studies argue that sorption of DSi occurs predominantly by aluminium and iron hydroxides (Huang et al., 2006; McKeague and Cline, 1963). Experiments with poisoned water showed that the removal of DSi began an hour after the experiment began (Bien et al., 1958).

This study quantifies the impact of salinization and freshening events in coastal aquifers under natural conditions on the dynamics of nutrients (the dissolved inorganic nitrogen (DIN = NO_3^-, NO_2^-, NH_4^+) and PO_4^{3-} and DSi). Trace elements such as Fe^{2+}, Mn^{2+} and boron were also studied in order to examine their effect on the behavior of the nutrients. This was accomplished by performing laboratory column experiments with aquifer sediments simulating salinization and freshening events under aerobic and anaerobic conditions. It should be noted that the goal of the experiments was to reproduce the processes occurring in the field (in the FSI zone) in order to understand them better; obtaining exact results was not necessarily anticipated, especially since the experiments examined nutrients which are sensitive parameters. To the best of our knowledge, laboratory simulations of nutrient dynamics under a wide range of salinities and redox conditions have never been conducted before.

2. Methods

2.1. Laboratory experiments

The experiments were conducted using aquifer sediments, fresh groundwater and seawater taken from two locations in Israel. The first location was the Poleg well near Netanya (Poleg) and the second was, the Nizzanim Sand Nature Reserve near Ashdod (Nizzanim). The sediments were sampled near the water table depth, which is in the oxic zone, so no special treatment was needed. Fresh groundwater was sampled from several meters below the water table depth by pumping, using a 1.5″ water-jet pump (Flojet). The Poleg well is located 70 m from the shoreline, above the intertidal zone, and thus sediment and fresh groundwater could be sampled from there. However, in Nizzanim there is no fresh groundwater in the intertidal zone but only at a higher location with a high water table depth (more than 10 m). Therefore, in Nizzanim the sediment was taken at a distance of 40 m from the shoreline, at a depth of 1.5–2 m, and fresh groundwater was pumped from an observation well located ~900 m from the shoreline using a submersible pump (Grundfos).

The sediments from the two sites are similar. The sediment from Poleg is fine-grained calcareous sand (mainly 0.2–0.4 mm), the dry weight consisting of 83 wt.% quartz , 15.3 wt.% calcium carbonate, 0.7 wt.% clay, 0.6 wt.% organic matter and 0.4 wt.% iron. The sediment from Nizzanim is coarser, with 0.7–0.9 mm sized particles consisting of 88 wt.% quartz, 10.8 wt.% calcium carbonate, 0.5 wt.% clay, 0.5 wt.% organic matter and 0.2 wt.% iron. The clay composition of the two sediments is mainly illite–smectite, secondary kaolinite and traces of chlorite.

Each experiment included three steps: (1) freshwater flow before the salinization experiment (preliminary stage); (2) replacing fresh groundwater with seawater (salinization); and (3)

replacing seawater with fresh water (freshening). Two experiments were conducted using seawater, fresh water and sediment from Poleg: the first performed without controlling the conditions of the water tank pumped into the column, i.e., under natural oxygen conditions (called "aerobic"), and the second under anaerobic conditions (called "anaerobic1"). The experiment in which fresh groundwater and sediment from Nizzanim were used was conducted under anaerobic conditions (called "anaerobic2"). The anaerobic conditions were established by purging N_2 gas, which contained an atmospheric level of CO_2 (~300 ppmv), into the water tank. The CO_2 was used in order to replace the original dissolved CO_2 that was removed from the water due to the purging. N_2 gas was chosen for the anaerobic conditions since it is inert. However, it can cause some increase of pH (Lee et al., 2010), which can explain the relatively high pH value found in the fresh groundwater (~8.1 compared with ~7.5 during the aerobic experiments). The anaerobic2 experiment was designed in order to repeat the anaerobic1 experiment under somewhat different conditions (e.g., higher P content), this time with more data gathering. Therefore, during the anaerobic2 experiment, all the experimental stages (the preliminary stage, salinization and freshening) continued for a longer time, i.e., to 10–20 pore volumes (PVs) compared to the 2–6 PVs of the aerobic and anaerobic1 experiments. Saturation indices (SIs) for aragonite, calcite and hydroxyapatite, during anaerobic2 experiment were calculated by PHREEQC code (Parkhurst and Appelo, 1999).

The experimental design is displayed in Fig. 1. The experimental column was 30 cm long with a 10 cm internal diameter packed with the sediment taken from the study area. The sediment was packed slowly by depositing small amounts of the original sand sample (with no prior drying) by spoon into thin layers (~1 cm) of water. This method is similar to the method described by Oliviera et al. (1996), but without using a wooden pestle or vibrating the column. The experimental solution (fresh groundwater or Mediterranean seawater) was pumped through the column with a peristaltic pump and proper tubing. The water flowing out from the column was inserted into a small vial (~5 mL) designed for constantly monitoring DO levels during the experiment by using a DO electrode (Multi 340i set, WTW). From the vial, the water flowed out through the tubes to be sampled.

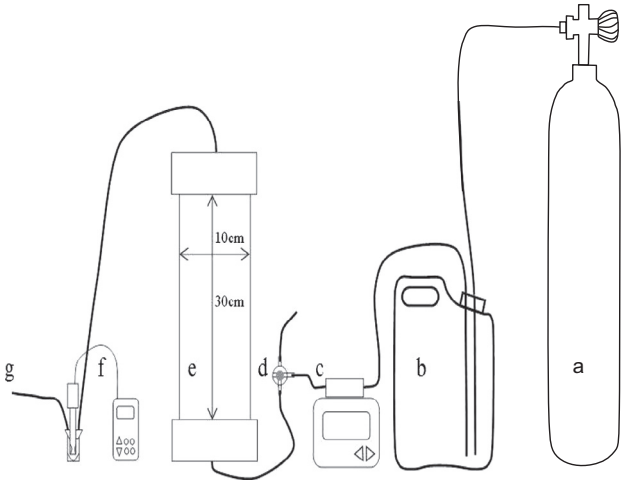

Fig. 1. Schematic diagram of the experimental design: Purging N_2 with 300 ppm CO_2 for creating anaerobic conditions (a); the end-members water tank (fresh groundwater or seawater) (b); peristaltic pump (c); a valve controlling the flow direction from the peristaltic pump to the column or to the sampling tube in order to sample the water tank (d); the sediment column (e); a small vial designed for constant electrode measuring of DO (f); and tubing for outflow of water for sampling (g).

The experiments were conducted at a flow rate of about 1 mL min^{-1}. This flow rate is equivalent to a velocity of about 200 m y^{-1}, which is one order of magnitude higher than the general groundwater velocity in the Israeli coastal aquifer. However, a previous experimental study (Russak and Sivan, 2010) in similar settings showed that the geochemical process of cation exchange is not significantly affected by such differences in flow velocities. This flow rate was chosen in order to make the duration of the experiments reasonable and avoid long-term "column effect" (such as preferential flow of the water in the side wall of the column). The experiments, in which water and sediment from Poleg were used (aerobic and anaerobic1 experiments), ran for a week, and the anaerobic2 experiment, in which water and sediment from Nizzanim was used, ran for a month.

Water flowing out of the vial was sampled regularly at predetermined periods. During the aerobic and anaerobic1 experiments, samples were taken continuously. During the anaerobic2 experiment samples were taken continuously only while the salinity changed from fresh water to seawater (or vice versa). For the duration of the rest of the experiment, samples were taken every few hours (3–5 times a day) due to the long extent of the experiments.

The volume of water sampled was about 50 mL, and each sample was divided into sub-samples using a 0.45 μm filter for different analyses: major ions; alkalinity; and nutrients (DIN species, PO_4^{3-} and DSi). Sub-samples of 20 mL were taken for analysis of the stable nitrogen and oxygen isotope ratio of NO_3^- ($\delta^{15}N$ and $\delta^{18}O$, respectively) during the two Poleg experiments (aerobic and anaerobic1). Sub-samples were taken for trace element analysis (Fe^{2+}, Mn^{2+} and boron) during the Nizzanim experiment (anaerobic2). Nitric acid (0.1 N) was added to the sub-samples for dissolved Fe^{2+} and Mn^{2+}. For an additional measurement of dissolved Fe^{2+} 1 mL was also fixed with Ferrozine (Stookey, 1970). All water samples were kept at 4 °C until analyzed, except for the nutrient and DIN isotope samples, which were frozen. Table 1 summarizes the analyses from each experiment.

2.2. Analytical methods

Major cations, SO_4^{2-}, Fe^{2+} and Mn^{2+} concentrations, were analyzed by inductively coupled plasma-atomic emission spectroscopy (ICP-AES, P-E optima 3300) with a precision of 2%. It should be noted that ICP-AES was used to determine the total element concentration and not the concentrations of ions. Nevertheless, a charge was added to the elements to emphasize that the charge controls the water/rock exchange process. Fe^{2+} was also measured by a spectrophotometer (Lambda2S, Elmer Perkins) after fixation with Ferrozine (Stookey, 1970). Total boron was analyzed by an inductively coupled plasma–mass spectrometer (ICP–MS) with a precision of 2%. Cl^- was measured by titration with a 0.01 N $AgNO_3$ solution, and low Cl^- concentration (below 100 meq L^{-1}) samples were analyzed by ion chromatography (Dionex 4000i). The errors calculated by averaging duplicate samples in both methods were less than 3%. Total alkalinity (ALK) was measured by titration (785 DMP Titrino, Metrohm) with 0.01 N HCl. The error calculated by averaging duplicate samples was ±0.03 meq L^{-1}.

Table 1
List of analyses for each of the experiments.

Experiment	Major ions	Nutrients	Isotope ratio	Trace elements
Aerobic	+	+	+	–
Anaerobic1	+	+	+	–
Anaerobic2	+	+	–	+

NO_3^-, NO_2^-, PO_4^{3-} and DSi concentrations were determined using the photo(spectro)metric method, either by Skalar SAN^{plus} or by LACHAT instruments' flow injection Quick-Chem 8500 auto-analyzer. It should be noted that in the pH of most aquatic systems, including the Israeli groundwater system, the main species of P are actually HPO_4^{2-} or H_2PO^{4-}, but they were considered as PO_4^{3-} for simplification. NH_4^+ was determined either by Skalar SAN^{plus} or by Aquafluor (Holmes et al., 1999). The detection limit of these methods is below 0.1 μM, with a precision of 5%. The accuracy of the analyses of the nutrients, major and trace elements was assured by including certified standards (by Merck).

The $\delta^{15}N$ and $\delta^{18}O$ in NO_3^- and in NO_2^- were determined using the azide method (McIlvin and Altabet, 2005). First, NO_3^- was reduced to NO_2^- using cadmium, then the NO_2^- was reduced to nitrous oxide using sodium azide, and then nitrous oxide was analyzed by GS-IRMS (Delta V Advantage by Thermo). For water sampled from the anaerobic experiment, an additional analysis of the $\delta^{15}N$ in NO_2^- was needed in order to achieve a precise calculation of $\delta^{15}N$ of NO_3^- ($\delta^{15}N_{NO3}$), due to the high concentration of NO_2^-. The precision of the GS-IRMS was 0.2‰ for $\delta^{15}N$ and 0.5‰ for $\delta^{18}O$, and the results reported are relative to Air and VSMOW, respectively. The errors from the standard deviation between duplicates were given for most of the samples analyzed for $\delta^{15}N$ and $\delta^{18}O$. The following international standards were combined into a samples batch: IAEA NO3 ($\delta^{15}N$ 4.7‰, $\delta^{18}O$ 25.6‰) USGS 32 + 34 ($\delta^{15}N$ 15‰, $\delta^{18}O$ −23.6‰), and the internal standards KNO_{3i} ($\delta^{15}N$ 1.3‰, $\delta^{18}O$ 14.1‰), $NaNO_{2i}$ ($\delta^{15}N$ −63‰) and $NaNO_{2ii}$ ($\delta^{15}N$ 2.7‰). Standards were measured before and after a set of samples in order to correct the readings. It should be noted that the $\delta^{15}N$ and $\delta^{18}O$ of seawater were not analyzed successfully due to the low concentration of NO_3^- in the seawater, and were estimated using data from Eliani-Russak et al. (2013), that indicated values for $\delta^{15}N$ (2.2‰ ± 0.2) and $\delta^{18}O$ (1.5‰ ± 0.5).

Particle-size distribution (PSD) analysis was conducted on sediment from Poleg using the laboratory sieve shaker method and a laser diffraction system (MS-2000, Malvern). PSD analysis of sediment from Nizzanim was conducted using another laser diffraction system (Analysette MicroTec plus). The clay percentage was determined by the pipette method, filtering the clay from a sediment sample based on Stokes' law. X-ray diffraction (XRD) was used in order to characterize the mineralogical and clay composition of the sediment. Calcium carbonate percentage was determined by the pressure calcimeter method (Loeppert and Suarez, 1996). Organic matter (OM) content was measured by the wet oxidation and titration methods (Tiessen and Moir, 1993). In addition, the chemical composition of the sediments was analyzed using $LiBO_2$ to dissolve the sediment and the analysis was made using ICP-AES. Sediment loss on ignition (LOI) was also analyzed.

3. Results

The nutrient results from the aerobic experiment and the two anaerobic experiments simulating salinization and freshening of the Israeli coastal aquifer are herewith presented. Average values of the end-members (fresh groundwater and seawater) are presented in Table 2 and all the data from the experiments are presented in the appendix (Table A1). The parameters are plotted in Figs. 2–7 as breakthrough curves versus the number of pore volumes (PVs), which are commonly used in column experiments (e.g., Appelo, 1994; Goren et al., 2011). One PV represents the total volume of water in the column (filling the pores between the sediment particles). If the measured parameter is conservative (as Cl^-), its concentration will be half of the eluent (the water entering the column) after 1 PV and shortly afterward (depending on the dispersion) it will reach the concentration of the eluent, indicating a full replacement of the original solution. Thus, PVs enable a comparison between the different experiments and between conservative and non-conservative behavior.

The breakthrough curves of nitrate and nitrite concentrations and isotopic values were compared to the expected conservative behavior calculated between the two end members (fresh groundwater and seawater). During the aerobic salinization and freshening experiments, NO_3^-, NO_2^-, $\delta^{15}N$ and $\delta^{18}O$ were nearly conservative (Fig. 2). During the anaerobic1 experiment, there was depletion in NO_3^- concentration and enrichment in NO_2^- concentration and in ^{15}N and ^{18}O, compared to the conservative behavior (Fig. 3). It should be noted that when the NO_3^- and NO_2^- concentrations were in the same range (when the salinity was high or when NO_2^- concentration was high) the $\delta^{18}O$ could be affected by the $\delta^{18}O$ in NO_2^-. For the nitrogen isotope ratio ($\delta^{15}N$) the effect from NO_2^- could be checked, since there were standards to measure the $\delta^{15}N$ in NO_2^-. Unfortunately, the real values of the $\delta^{18}O$ in NO_3^- could not be calculated due to the lack of standards for measuring the $\delta^{18}O$ in NO_2^-.

The oxygen isotopes ratio ($\delta^{18}O$) during the anaerobic1 freshening could be affected by the $\delta^{18}O$ in NO_2^- since it is in the same concentration scale as NO_3^-. For the nitrogen isotope ratio ($\delta^{15}N$) we were able to check the effect from NO_2^-, as we had standards to measure the $\delta^{15}N$ in NO_2^-. Unfortunately, without standards for the $\delta^{18}O$ in aNO_2^- the true values of the $\delta^{18}O$ in NO_3^- could not be calculated.

Similar trends of depletion in NO_3^- concentration and enrichment of NO_2^- concentration occurred during the second anaerobic experiment (anaerobic2; Fig. 4). It seems that whenever the water salinity was low, the NO_3^- concentration was lower than expected from conservative behavior (green dashed line in Fig. 4). On the other hand, the NO_2^- concentration was higher than expected. This inverse trend of NO_3^- and NO_2^- was obvious in the preliminary stage (of the freshwater flow, before the salinization experiment, Fig. 4a). It should be noted that after about 5 PVs, the concentration of the NO_2^- decreased, even though the NO_3^- concentration continued to decrease (Fig. 4a). The DO concentration during the anaerobic2 experiment decreased from 4 mg L^{-1} in the beginning of the preliminary stage to below 0.1 mg L^{-1} after 5 PVs (Fig. A1 in the appendix). This low value of DO levels was constant during the anaerobic2 experiment, except for a somewhat higher concentration during the salinization experiment, up to 1.2 mg L^{-1}, at about 9 PVs (which then decreased again). The pH values were in the range of 7–8 during the anaerobic2 experiment.

Ammonium concentrations during the aerobic salinization experiment fluctuated within the end member values (0–1 μmol L^{-1}, Fig. 5a). During the anaerobic1 salinization, NH_4^+ concentrations increased to a maximum value of about 80 μmol L^{-1}, higher than the end members by about two orders of magnitude (Fig. 5a). During the aerobic and anaerobic1 experiments, the PO_4^{3-} concentration increased to a higher concentration than that observed in seawater (Fig. 5b). The enrichment began at approximately the same time (∼1 PV) in both experiments; however, the peak amplitude was different. After reaching those peaks, PO_4^{3-} concentrations remained relatively constant until the end of the experiments (2.5 and 2 PVs, respectively, Fig. 5b).

Freshwater concentrations of PO_4^{3-} in the anaerobic2 experiment were relatively high, ∼120 μmol L^{-1} (Fig. 6a). During the beginning of the preliminary stage of the experiment, the PO_4^{3-} concentration was much lower than in the freshwater that entered the column, and it increased gradually until it reached freshwater values at 9 PVs (Fig. 6a). During the anaerobic2 salinization experiment, PO_4^{3-} concentrations increased and reached a maximum value of ∼180 μmol L^{-1} at about 1.5 PV and then decreased (Fig. 6b). Nevertheless, even after 11 PVs, the concentration of PO_4^{3-} was well above that of seawater (20 versus 1–2 μmol L^{-1},

Table 2
Chemical composition of the end member from the experiments.

[Av. ± Std (n)] Experiment	meq/L Na^+	meq/L K^+	meq/L Mg^{2+}	meq/L Ca^{2+}	meq/L Sr^{2+}	meq/L Cl^-	meq/L SO_4^{2-}	mmol/L ALK
Majors								
FW-Small	17 ± 0 (6)	0.3 ± 0.0 (6)	4.0 ± 0.0 (6)	4.9 ± 0.1 (6)	0.046 ± 0.001 (6)	22 ± 0 (6)	2.0 ± 0.0 (6)	2.46 (1)
SW-Small	542 ± 6 (5)	13.8 ± 1.8 (5)	124 ± 1 (5)	22.9 ± 0.7 (5)	0.200 ± 0.008 (5)	640 ± 5 (5)	65 ± 1 (5)	2.88 ± 0.08 (2)
FW-Aer	24 ± 1 (2)	0.4 ± 0.1 (2)	5.1 ± 0.1 (2)	7.3 ± 0.3 (2)	0.072 ± 0.001 (6)	31 ± 0 (2)	3.1 ± 0.1 (2)	2.61 ± 0.01 (7)
SW-Aer	544 ± 6 (4)	12 ± 1 (4)	126 ± 2 (4)	24 ± 1 (4)	0.198 ± 0.005 (4)	643 ± 8 (4)	66 ± 2 (2)	2.70 ± 0.01 (4)
FW-Ana1	24 ± 2 (2)	0.5 ± 0 (2)	5.6 ± 0.3 (2)	4.3 ± 0.1 (2)	0.039 ± 0.001 (2)	29 ± 2 (2)	3.0 ± 0.1 (2)	2.75 ± 0.03 (3)
SW-Ana1	546 ± 2 (2)	12 ± 1 (2)	124 ± 1 (2)	24 ± 0 (2)	0.196 ± 0.001 (2)	653 ± 3 (2)	66 ± 0 (2)	2.76 ± 0.03 (3)
FW1-Ana2	4.8 ± 0.0 (2)	0.2 ± 0.0 (2)	2.0 ± 0.0 (2)	3.8 ± 0.0 (2)	0.025 ± 0.000 (2)	4.5 ± 0.0 (3)	0.7 ± 0.1 (2)	5.46 ± 0.02 (3)
SW-Ana2	520 ± 13 (3)	12 ± 1 (3)	119 ± 2 (3)	24 ± 2 (3)	0.197 ± 0.025 (3)	634 ± 7 (3)	64 ± 1 (2)	2.79 ± 0.01 (5)
FW2-Ana2	2.2 ± 0.0 (2)	0.1 ± 0.0 (2)	1.3 ± 0.1 (2)	3.5 ± 0.1 (2)	0.026 ± 0.003 (2)	2.2 ± 0.1 (4)	0.4 ± 0.1 (2)	4.44 ± 0.04 (6)

[Av. ± Std (n)] Experiment	µmol/L NO_3^-	µmol/L NO_2^-	µmol/L NH_4^+	µmol/L PO_4^{3-}	µmol/L DSi	pH
Nutrients (and pH)						
FW-Aer	120 ± 40 (3)	0.3 ± 0.2 (4)	0.5 ± 0.4 (4)	0.4 ± 0.4 (3)	145 ± 15 (2)	7.2 ± 0.3 (4)
SW-Aer	1.7 ± 1.5 (4)	0.5 ± 0.1 (4)	0.4 ± 0.4 (3)	0.4 ± 0.3 (4)	5 ± 1 (4)	8.0 ± 0.0 (4)
FW-Ana1	74 ± 8 (2)	0.5 (1)	0.2 ± 0.1 (2)	0.1 ± 0.1 (3)	85 ± 8 (2)	N.A.
SW-Ana1	2.2 ± 1.3 (3)	0.8 ± 0.3 (3)	0.6 ± 0.6 (3)	0.7 ± 0.4 (3)	4.5 ± 0.6 (3)	7.9 ± 0.0 (2)
FW1-Ana2	275 ± 25 (4)	0.9 ± 0.1 (2)	0.1 (1)	107 (1)	300 ± 38 (4)	8.2 ± 0.1 (3)
SW-Ana2	1.6 ± 1.4 (4)	0.5 ± 0.3 (4)	0.3 (1)	3 ± 2 (4)	5.6 ± 0.8 (3)	7.9 ± 0.1 (5)
FW2-Ana2	166 ± 17 (6)	1.5 ± 0.8 (2)	0.1 ± 0.0 (2)	117 ± 21 (4)	275 ± 26 (6)	8.1 ± 0.0

[Av. ± Std (n)] Experiment	µeq/L Fe^{2+}[a]	µeq/L Mn^{2+}	µeq/L Ba^{2+}	µeq/L Li^+	µmol/L B	meq/L Br^-
Traces						
FW1-Ana2	<0.36 (3)	0.47 ± 0.24 (3)	40 ± 7 (3)	0.6 ± 0.0 (2)	11.9 ± 0.1 (2)	0.007 ± 0.001 (2)
SW-Ana2	0.6 ± 0.4 (3)	0.12 ± 0.08 (3)	10 ± 0.0 (3)	27 ± 3 (3)	430 ± 15 (3)	0.850 ± 0.072 (3)
FW2-Ana2	<0.36 (3)	0.75 ± 0.04 (3)	47 ± 2 (3)	0.4 ± 0.0 (2)	7 (1)	0.005 (1)

The number in brackets referred to the number of samples.
[a] The concentration of Fe^{2+} in the fresh water and in two samples from the seawater were below the detection limit (D.L) of Fe^{2+} (D.L = 0.36 µeq L^{-1}).

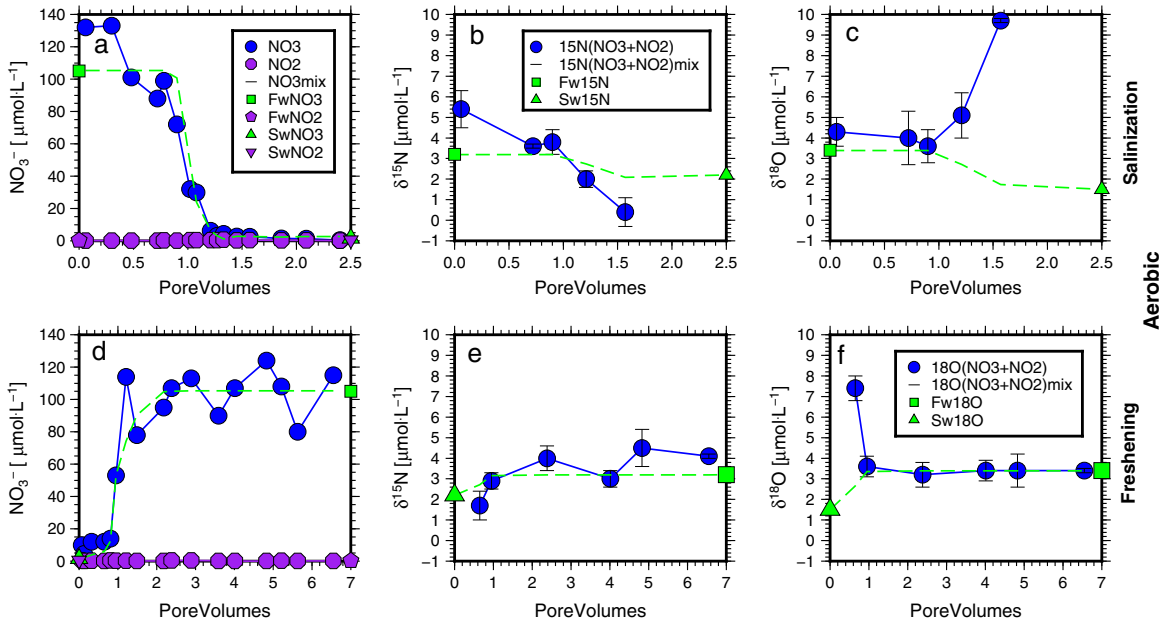

Fig. 2. Breakthrough curves of NO_3^- (blue circle) and NO_2^- (purple octagon) (a,d), $\delta^{15}N$ (blue circle) (b,e) and $\delta^{18}O$ (blue circle) (c,f) results from aerobic experiments (salinization and freshening) from the column outlet. The green dashed line represents the expected concentration of NO_3^-, $\delta^{15}N$ and $\delta^{18}O$ from mixing between the fresh water (FW, green square) and seawater (SW, green triangle). The concentrations of NO_2^- in the sources (water tanks) of fresh water and seawater are plotted as purple pentagons and inverse triangles, respectively. (For interpretation of the references to colour in this figure legend, the reader is referred to the web version of this article.)

respectively). During the anaerobic2 freshening experiment, PO_4^{3-} concentration did not exceed 50 µmol L^{-1} and was around 20 µmol L^{-1} during most of the experiment, much lower than the freshwater end member (Fig. 6c).

In the anaerobic2 experiment, the DSi concentration was depleted during the preliminary stage and during the freshening experiment, and was enriched during the salinization experiment (Fig. 7). DSi behavior during the aerobic and anaerobic1 experiments is displayed in Fig. A2 (in the appendix). In the anaerobic1 experiment, the DSi was enriched and remained nearly constant, within the range of the freshwater concentration. In the aerobic salinization experiment, the DSi was less enriched and showed depletion during the following freshening experiment.

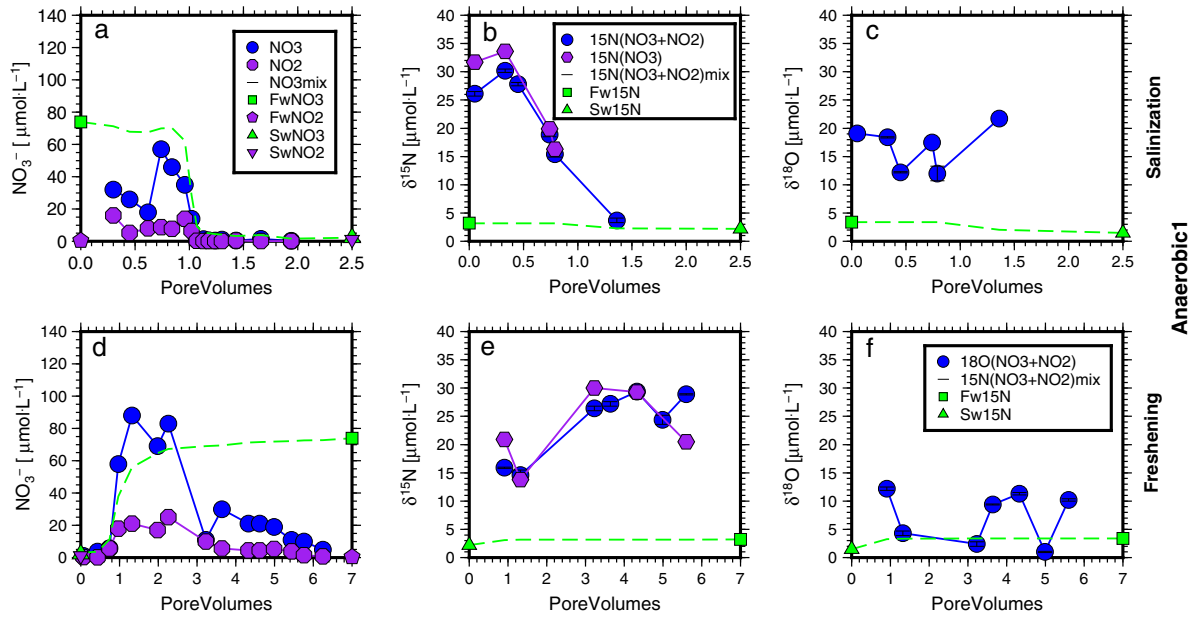

Fig. 3. Breakthrough curves of NO_3^- (blue circle) and NO_2^- (purple octagon) (a,d), $\delta^{15}N$ (blue circle) (b,e) and $\delta^{18}O$ (blue circle) (c,f) results from anaerobic1 experiments (salinization and freshening) from the column outlet. The green dashed line represents the expected concentration of NO_3^-, $\delta^{15}N$ and $\delta^{18}O$ from mixing between the fresh water (FW, green square) and seawater (SW, green triangle). The concentrations of NO_2^- in the sources (water tanks) of fresh water and seawater are plotted as purple pentagons and inverse triangles, respectively. Note that the $\delta^{15}N$ values of NO_3^- ($\delta^{15}N_{(NO3)}$) are plotted as well (purple hexagon). (For interpretation of the references to colour in this figure legend, the reader is referred to the web version of this article.)

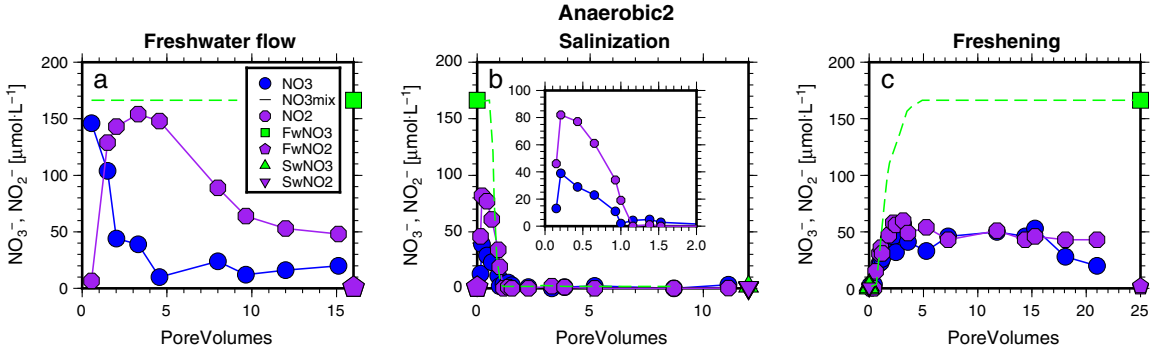

Fig. 4. Breakthrough curve of NO_3^- (blue circle) and NO_2^- (purple octagon) during anaerobic2 experiments: freshwater flow (preliminary stage) (a), salinization (b) and freshening (c) from the column outlet. The green dashed line represents the expected concentration of NO_3^- from mixing between the fresh water (FW, green square) and seawater (SW, green triangle). The concentrations of NO_2^- in the sources (water tanks) of fresh water and seawater are plotted on the *Y* axis as purple pentagons and inverse triangles, respectively. The small graph in the salinization graph (b) is a zoom-into the two first pore volumes. (For interpretation of the references to colour in this figure legend, the reader is referred to the web version of this article.)

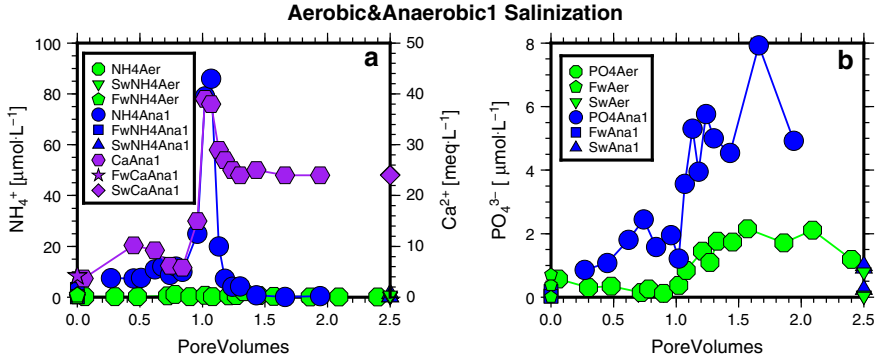

Fig. 5. Breakthrough curve of NH_4^+ from the aerobic (green pentagon) and of NH_4^+ (blue circle) and Ca^{2+} (purple hexagon) from the anaerobic1 salinization experiments (a) and breakthrough curve of PO_4^{3-} from the aerobic (green octagon) and anaerobic1 (blue circle) salinization experiments (b) from the column outlet. The fresh water (FW) and seawater (SW) concentrations of Ca^{2+} (purple star and diamond, respectively) and NH_4^+ and PO_4^{3-} in aerobic (green pentagon and inverse triangle, respectively) and anaerobic1 experiment (square and triangle, respectively). (For interpretation of the references to colour in this figure legend, the reader is referred to the web version of this article.)

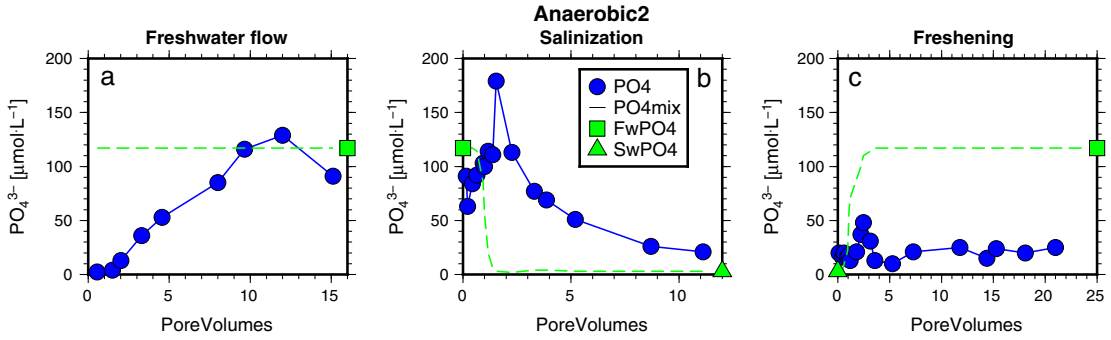

Fig. 6. Breakthrough curve of PO_4^{3-} from the anaerobic2 experiment: freshwater flow (preliminary stage) (a); salinization (b); and freshening (c) from the column outlet. Plotted on the *Y* axis are the concentrations of PO_4^{3-} in the sources (water tanks) of fresh water (FW, square) and seawater (SW, triangle). The green dashed line represents the expected concentration of PO_4^{3-} from mixing between the fresh water and seawater. (For interpretation of the references to colour in this figure legend, the reader is referred to the web version of this article.)

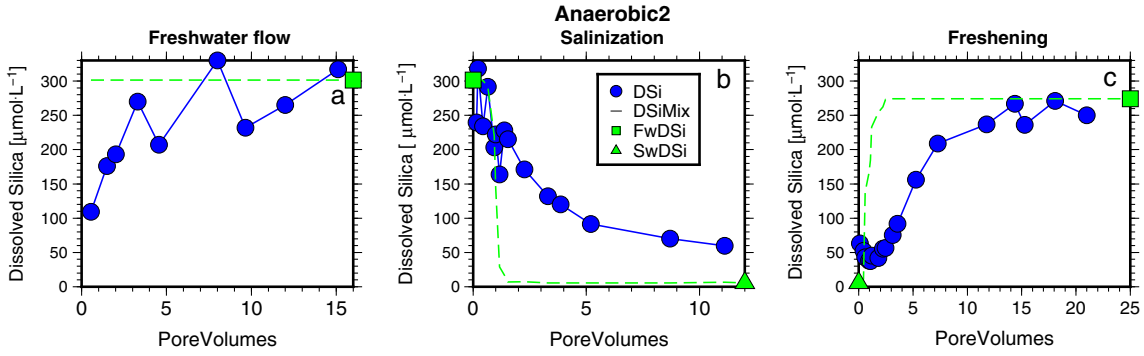

Fig. 7. Breakthrough curve of dissolved silica (DSi) from the anaerobic2 experiment: freshwater flow (preliminary stage) (a); salinization (b); and freshening (c) from the column outlet. Plotted on the *Y* axis are the concentrations of DSi in the sources (water tanks) of fresh water (FW, square) and seawater (SW, triangle). The green dashed line represents the expected concentration of DSi from mixing between the freshwater and seawater. (For interpretation of the references to colour in this figure legend, the reader is referred to the web version of this article.)

4. Discussion

The results of the column experiments show that the nutrients are affected by several geochemical and biological processes when fresh groundwater is replaced by seawater and vice versa. The water and the sediment used in the experiments were the natural sediment, fresh groundwater and seawater from the study area. In addition, the experiments were conducted under similar natural conditions prevailing in the aquifer (aerobic and anaerobic conditions). Thus, we believe that the experiments simulated the natural conditions in the fresh–saline interface of coastal aquifers well. In general, the switch from fresh groundwater to seawater and vice versa induces cation exchange affecting NH_4^+, anion exchange affecting PO_4^{3-} and DSi, and anaerobic processes affecting mainly NO_3^- and NO_2^-. The following sections discuss the processes involved.

4.1. Cation exchange

Cation exchange is a well-known process in the FSI, controlling the major cations (e.g., Appelo et al., 1990; Russak and Sivan, 2010). Regarding the DIN system, it was shown that NH_4^+ tends to adsorb in freshwater more than in saline water (e.g., Appelo et al., 1990; Seitzinger et al., 1991).

The NH_4^+ concentration displayed the same enrichment trend during the anaerobic1 salinization as Ca^{2+} (Fig. 5a, blue circles and purple hexagons, respectively), showing a high peak at the same time (~1 PV). Thus, the NH_4^+ enrichment was probably due to cation exchange. This result is consistent with the increased NH_4^+ documented during the salinization experiment of Appelo et al. (1990). During the aerobic salinization experiment, NH_4^+ concentrations remained low (green octagons in Fig. 5a). The lack of NH_4^+ concentration enrichment could be due to oxidation through nitrification, even though no clear evidence for NO_3^- or NO_2^- production was found to support this interpretation (Fig. 2a).

4.2. Anion exchange

Adsorption and desorption of PO_4^{3-} has been discussed in the literature (e.g., De Kanel and Morse, 1978; Goldberg, 1997). However, the effect of seawater intrusion on PO_4^{3-} was mentioned less frequently (e.g., Sivan et al., 2005; Stuyfzand, 1993). Only Price et al. (2010) showed in a column experiment that PO_4^{3-} was desorbed from the sediment during the replacement of distilled water by seawater, which they attributed to the competition with HCO_3^- on adsorption sites. The current study showcases the dynamics of PO_4^{3-} in a broader way, since it compares PO_4^{3-} concentrations with additional parameters such as DSi and boron and not just to HCO_3^-.

The similarity in the enrichment trends of the PO_4^{3-} concentrations during both the aerobic and anaerobic1 salinization (Fig. 5b) experiments and the anaerobic2 salinization experiment (Fig. 6b), beginning after about 1 PV, indicates that the enrichment of the PO_4^{3-} concentration does not depend on the concentration of the fresh groundwater (Table 2). The slow decrease in the PO_4^{3-} concentration after about 2.5 PVs suggests that the aerobic and anaerobic1 salinization experiments ended before the decrease in PO_4^{3-} concentration started, as they lasted less than 2.5 PVs.

Mass balance was calculated in order to compare the depletion observed during the preliminary stage (Fig 6a) and freshening (Fig. 6c) and the enrichment observed during salinization (Fig. 6b). The amount of PO_4^{3-} adsorbed or desorbed was evaluated by calculating the difference between the expected concentration of PO_4^{3-} following a conservative behavior (green dashed line in the figures) and the actual measured concentration during the preliminary stage, salinization and freshening experiments. It was found that the amount of PO_4^{3-} adsorbed during the preliminary stage was 400 μmol, similar to the amount of PO_4^{3-}, 380 μmol, desorbed during salinization. Thus, PO_4^{3-} release during anion exchange explains most of the PO_4^{3-} enrichment during salinization. However, the amount of PO_4^{3-} adsorbed during freshening was much higher, 1350 μmol. The higher depletion of PO_4^{3-} observed during freshening compared to the enrichment trend observed during salinization could be explained by the high adsorption affinity of PO_4^{3-} or by additional processes that affect PO_4^{3-}, which are elaborated below.

During the final part of freshening (9–21 PVs), alkalinity (ALK) and PO_4^{3-} showed a relatively constant decrease by about 200 and 100 μmol L^{-1}, respectively (Fig. 8b). The ALK trend most probably stems from constant precipitation of $CaCO_3$, which provides "new" adsorption sites for PO_4^{3-}, explaining at least part of the observed PO_4^{3-} depletion. PO_4^{3-} may have decreased also due to precipitation of hydroxyapatite given that the freshwater concentration of PO_4^{3-} exceeded 50 μmol L^{-1}, the minimum concentration for its precipitation (Sø et al., 2011). It should be noted that SI calculations for aragonite, calcite and hydroxyapatite for Ca^{2+}, ALK and PO_4^{3-} concentrations in the PV range between 5 and 21 yielded SI in the range of 0.2–0.4 for aragonite, 0.3–0.6 for calcite and 2–5 for hydroxyapatite. When calculated using their expected conservative concentrations the SIs were much higher: 0.5–0.6 for aragonite, 0.7–0.8 for calcite and 7 for hydroxyapatite. This also suggests that the pH in our experiments was controlled by calcium carbonate precipitation/dissolution and not by biogeochemical processes.

The depletion in DSi (relative to the expected) during the preliminary stage, its enrichment during the salinization experiment and its depletion again during the freshening experiment (Fig. 7) suggest the DSi was controlled by intense exchange during the aerobic and anaerobic1 experiments (Fig. A2). The enrichment and depletion of the DSi concentrations during the aerobic and anaerobic1 experiments (Fig. A2) were less obvious than during the anaerobic2 experiment (Fig. 7). However, an exchange process probably affected the DSi in these experiments. Moreover, no clear change in the DSi concentration during the anaerobic1 experiment could be connected to the high DSi concentration observed at the end of the salinization experiment (Fig. A2d).

Mass balance calculation of the DSi desorbed from the sediment during the anaeronic2 salinization experiment (11 PV) resulted in about 540 μmol. Taking into account that the DSi concentration did not decrease to that of seawater concentration, and assuming that the decrease was linear (Fig. 7b), the DSi should have reached seawater concentration at 21 PV. This would enable calculation of an additional desorption of 140 μmol of DSi, which amounts to 680 μmol. This is in the range of the amount of DSi adsorbed on the sediment during the preliminary stage (460 μmol) and during the freshening experiment (830 μmol). In previous studies, enrichment of the DSi during seawater intrusion was explained by the dissolution of biogenic silica (e.g., Miretzky et al., 2001); here we show, however, that the major process affecting silica is exchange. It should be noted that DSi exchange was mentioned in the context of artificial groundwater recharge (e.g., Wood and Signor, 1975; Stuyfzand, 1998).

The enrichment of PO_4^{3-} and DSi during salinization and their depletion during freshening indicate that they were affected by anion exchange. Possible candidates for exchange are boron and ALK, because they show an opposite trend to that of PO_4^{3-} and DSi when plotting the difference in the concentrations between their measured and expected (from conservative behavior) values during the experiments (Fig. 8). While ALK in the rather low pH range (7–8) of the anaerobic2 experiment is mainly the anion HCO_3^- (Stumm and Morgan, 1996), DSi and boron are predominantly at their non-ionic states of $Si(OH)_4$ and $B(OH)_3$ (Stumm and Morgan, 1996; Appelo and Postma, 1996). This does not significantly affect the ion exchange efficiency of boron and DSi because the non-ionic species may associate/dissociate to account for their adsorbed/desorbed ionic species (Brinkman, 1993; Keren and Mezuman, 1981; Obihara and Russell, 1972).

Figure 8a shows that during salinization boron indeed has an opposite trend to that of PO_4^{3-} and DSi, suggesting that boron is adsorbed in the exchange with PO_4^{3-} and DSi. However, the depletion of the boron concentration is too small to compensate for the enrichment of the PO_4^{3-} and DSi concentrations. While each of the PO_4^{3-} and DSi concentrations were enriched at most by 180 and 210 μmol L^{-1}, respectively, the maximum depletion of boron concentration was only 170 μmol L^{-1}. Moreover, boron reached its seawater concentration after 3 PVs, whereas the PO_4^{3-} and DSi concentrations were enriched even at the end of the experiment (after 11 PVs). Since during salinization ALK showed depletion at PV = 1.7, when the boron concentration was already recovering, it

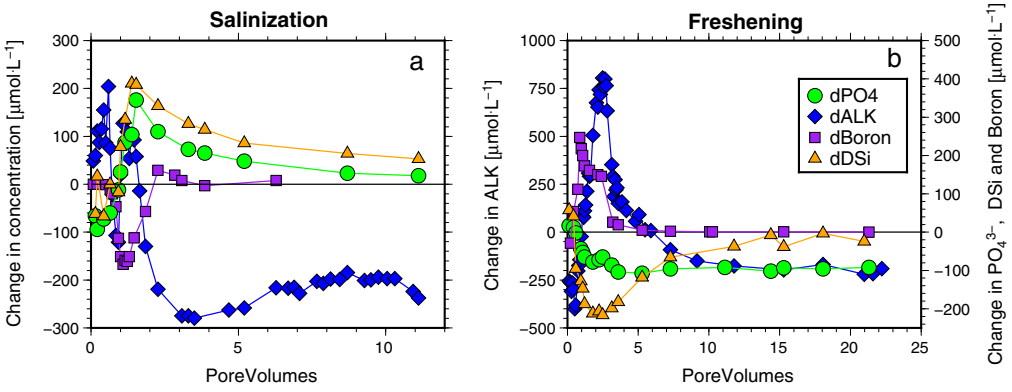

Fig. 8. Change in alkalinity (ALK, blue), PO_4^{3-} (green), dissolved silica (DSi, orange) and boron (purple) during anaerobic2 experiment: salinization (a); and freshening (b). The peaks of PO_4^{3-} and DSi during salinization correlate with depletions in boron and ALK. During freshening depletions of PO_4^{3-} and DSi correlate with the peak of boron. After 5 PV, PO_4^{3-} and ALK are depleted at considerably constant amounts. (For interpretation of the references to colour in this figure legend, the reader is referred to the web version of this article.)

implies that ALK has a role in the exchange process. However, it is impossible to calculate the actual amount of HCO_3^- (ALK) that balances the enrichment of PO_4^{3-} and DSi, since other processes, such as precipitation/dissolution of $CaCO_3$, may also affect the ALK. Precipitation of $CaCO_3$ was indicated in the experiments by the steady state ALK difference (from PV 6, Fig. 8a), which was 0.2 mmol L^{-1} lower than that of inflowing seawater (2.6 mmol L^{-1} versus 2.8 mmol L^{-1}, respectively).

During the freshening experiment, boron concentration showed enrichment while concentrations of PO_4^{3-} and DSi showed depletion (Fig. 8b). However, boron concentration was enriched only during the first 3.5 PVs, whereas PO_4^{3-} and DSi concentrations were depleted for almost the entire experiment (21 PVs). It appears, therefore, that boron was not the only constituent exchanging with PO_4^{3-} and DSi during the experiment. We checked the possibility that also ALK exchanged with PO_4^{3-} and DSi. The ALK showed a considerable enrichment of up to 800 mmol L^{-1} during the initial part of the freshening experiment (1–5 PVs). This value exceeds the amount needed to balance the depletion of PO_4^{3-} and DSi, and may stem from dissolution of calcium carbonate. SI calculations for the range 1.5–3.5 PV show that the water was almost saturated with respect to $CaCO_3$ minerals (SI of −0.2 to 0.2 for aragonite and −0.05 to 0.2 for calcite). This indicates that the observed depletion in Ca^{2+} (due to adsorption, e.g., Appelo et al., 1990; Russak and Sivan, 2010) should have triggered the $CaCO_3$ dissolution resulting in the observed ALK enrichment.

4.3. Anaerobic processes

The depletion of NO_3^- and the enrichment of NO_2^- during all the anaerobic experiments (Figs. 3a, d and 4) are attributed to denitrification. This process is supported by the anoxic conditions and the high values of the isotopic ratios of nitrogen ($\delta^{15}N$) observed during the anaerobic1 experiment (Fig. 3b and e). The results of the NO_3^- and NO_2^- from the anaerobic1 salinization experiment showed that denitrification occurred even before the salinization experiment, during the freshwater flow and at the freshening experiment.

The results of the NO_3^- and NO_2^- concentrations from the anaeronic2 experiment showed the same trend and thus support the interpretation of the anaerobic1 experiment results, i.e., that denitrification occurred (Fig. 4). The initial 5 PVs of the preliminary stage (the freshwater flow, before the salinization experiment) display most clearly the opposite trends of the NO_3^- and NO_2^- concentrations, which occurred due to denitrification (Fig. 4a). Indeed, the dissolved oxygen during most of the anaerobic2 experiment was low enough to support denitrification (Fig. A1). During the preliminary stage, the DO level rapidly decreased during the 5 PVs at a similar rate to the decrease in the NO_3^- concentration (Figs. A2a and 4a, respectively). This supports the theory that denitrification could occur during the anaerobic experiments.

During the anaerobic2 preliminary stage, the NO_2^- concentration began to decrease even though the NO_3^- concentration continued to decrease (Fig. 4a). This could be explained if the rate of the second step of denitrification, i.e., reduction of NO_2^- to NO had increased (NO reduces to N_2O and finally to N_2). The decrease in NO_2^- concentration could theoretically be due to anammox, when NO_2^- and NH_4^+ are consumed and N_2 is produced. However, in our experiment neither anammox nor DNRA should be of any relevance, since the study area has a low organic matter content. Moreover, during the preliminary stage, the NH_4^+ did not reach a concentration higher than 1 μmol L^{-1}.

The results indicate that denitrification can occur rapidly in the FSI and below the FSI, provided there is a low DO concentration and a supply of NO_3^-. These conditions exist below the FSI of many coastal aquifers (e.g., Addy et al., 2005; Charette, 2007), where the saline groundwater is under anoxic conditions and NO_3^- is supplied from the fresh groundwater. In the current study, the denitrification seemed to occur only when the salinity of the water was low, in the range of the freshwater with its high concentration of NO_3^-. Thus, NO_3^- depletion was observed during the preliminary stage and at the beginning of the salinization experiment, before the salinity increase. Denitrification was also indicated during the freshening, when the water salinity exiting the column reached that of freshwater. When the water became more saline, during the salinization experiment, there was no evidence for denitrification and the NO_3^- seemed to remain conservative (Figs. 3a and 4b). Moreover, during the anaerobic1 freshening experiment, the denitrification began after 3 PVs, while between 1 and 2.25 PVs the NO_3^- was high (Fig. 3d). This implies that the denitrifiers were not active under higher salinity values, and they probably needed some time after the seawater flow before they could use the NO_3^- for denitrification. The sediment for the experiments was taken from the shallow oxidized depth, which could explain why in our experiments denitrification occurred only when the sediment was flushed by fresh groundwater, whereas deeper in the aquifer, in the suboxic FSI zone, the denitrifiers are probably more active.

It seems that the anaerobic respiration in the system studied was limited to denitrification since NO_3^- was not completely exhausted. In addition, during the anaerobic2 experiments Mn^{2+} concentrations were not higher than 0.5 μmol L^{-1}, Fe^{2+} concentrations were below detection limit and the sulfur stable isotope ratio ($\delta^{34}S$) was no different than that of seawater. Therefore, there was no evidence for anaerobic respiration using manganese, iron or sulfate.

5. Conclusions

This study demonstrates that seasonal fluctuations in salinity and dissolved oxygen in coastal aquifers may control the nutrient distribution in groundwater. The salinization and freshening experiments in this study showed that NH_4^+ and PO_4^{3-} and DSi were affected mainly by ion exchange processes while microbial activity controlled the nitrogen species NO_3^- and NO_2^-. The PO_4^{3-} and DSi were exchanged with HCO_3^- and boron; this, however, depends on the composition of groundwater and sediments of the aquifer. Salinization under anaerobic conditions results in NH_4^+ enrichment due to desorption, while denitrification in anaerobic salinization and freshening is the major process reducing NO_3^- and increasing NO_2^- and the $\delta^{15}N$ of NO_3^- by 15–25‰. During aerobic conditions, NO_3^- and NO_2^- behave conservatively. During aerobic salinization NH_4^+ is probably released by cation exchange and then removed biologically by nitrification.

Acknowledgements

We would like to thank H. Hemo, S. Ashkenazi and I. Swaed from the Israeli Geological Survey for their help in the field. We also thank O. Yoffe, D. Stibler, O. Goren, O. Crouvi, A. Sandler and Y. Boaz from the Israeli Geological Survey, E. Shani, O. Bialik, G. Biran and E. Eliani-Russak from the Ben Gurion University, K. Yanuka and Y. Segal from the Oceanographic and Limnological Research and T. Rivlin from the Inter-University Institute for Marine Science for their help with sample analyses. Special thanks go to N. Knossow, Y. Sadeh and R. Algon from the Ben Gurion University for helping to conduct the experiments and to S. Shani-Kadmiel from the Ben Gurion University for helping to design the figures. This research was supported by the Israel Science Foundation (OS #857/09) and the Water Authority (OS and YY).

Appendix A. Supplementary material

Supplementary data associated with this article can be found, in the online version, at http://dx.doi.org/10.1016/j.jhydrol.2015.07.034.

References

Addy, K., Gold, A., Nowicki, B., McKenna, J., Stolt, M., Groffman, P., 2005. Denitrification capacity in a subterranean estuary below a Rhode Island fringing salt marsh. Esturies 28, 896–908.

Altabet, M.A., Pilskaln, C., Thunell, R., Pride, C., Sigman, D., Chavez, F., Francois, R., 1999. The nitrogen isotope biogeochemistry of sinking particles from the margin of the Eastern North Pacific. Deep-Sea Res. I 46, 655–679.

Andersen, M.S., Nyvang, V., Jakobsen, R., Postma, D., 2005. Geochemical processes and solute transport at the seawater/freshwater interface of a sandy aquifer. Geochim. Cosmochim. Acta 69, 3979–3994.

Appelo, C.A.J., 1994. Cation and proton exchange, pH variations, and carbonate reactions in a freshening aquifer. Water Resour. Res. 30, 2793–2805.

Appelo, C.A.J., Postma, D., 1996. Geochemistry, Groundwater and Pollution. A.A. Balkema.

Appelo, C.A.J., Willemsen, A., Beekman, H.E., Griffioen, J., 1990. Geochemical calculations and observations on salt water intrusions. II. Validation of a geochemical model with laboratory experiments. J. Hydrol. 120, 225–250.

Baldwin, D.S., Rees, G.N., Mitchell, A.M., Watson, G., Williams, J., 2006. The short-term effects of salinization on anaerobic nutrient cycling and microbial community structure in sediment from a freshwater wetland. Wetlands 26, 455–464.

Bear, F.E., 1964. Chemistry of the Soil, second ed. Van Nostrad Reinhold Company, New York.

Beekman, H.E., Appelo, C.A.J., 1991. Ion chromatography of fresh- and salt-water displacement: laboratory experiments and multicomponent transport modeling. J. Contam. Hydrol. 7, 21–37.

Bien, G.S., Contois, D.E., Thomas, W.H., 1958. The removal of soluble silica from fresh water entering the sea. Geochim. Cosmochim. Acta 14, 35–54.

Brinkman, A.G., 1993. A double-layer model for ion adsorption onto metal oxides, applied to experimental data and to natural sediments of Lake Veluwe, The Netherlands. Hydrobiologia 253, 31–45.

Casciotti, K.L., Sigman, D.M., Hastings Galanter, M., Bohlke, J.K., Hilkert, A., 2002. Measurement of the oxygen isotopic composition of nitrate in seawater and freshwater using the denitrifier method. Anal. Chem. 74, 4905–4912.

Charette, M.A., 2007. Hydrologic forcing of submarine groundwater discharge: insight from a seasonal study of radium isotopes in a groundwater-dominated salt marsh estuary. Limnol. Oceanogr. 52, 230–239.

Charette, M.A., Sholkovitz, E.R., Hansel, C.M., 2005. Trace element cycling in a subterranean estuary: Part 1. Geochemistry of the permeable sediments. Geochim. Cosmochim. Acta 69, 2095–2109.

Cline, J.D., Kaplan, I.R., 1975. Isotopic fractionation of dissolved nitrate during denitrification in the Eastern Tropical North Pacific Ocean. Mar. Chem. 3, 271–299.

Dalsgaard, T., Canfield, D.E., Petersen, J., Thamdrup, B., Acuña-González, J., 2003. N_2 production by the anammox reaction in the anoxic water column of Golfo Dulce, Costa Rica. Nature 422, 606–608.

De Kanel, J., Morse, J.W., 1978. The chemistry of orthophosphate uptake from seawater on to calcite and aragonite. Geochim. Cosmochim. Acta 42, 1335–1340.

Eliani-Russak, E., Herut, B., Sivan, O., 2013. The role of highly stratified nutrient-rich small estuaries as a source of dissolved inorganic nitrogen to coastal seawater, the Qishon (SE Mediterranean) case. Mar. Pollut. Bull. 71, 250–258.

Fonseca, R., Canário, T., Morais, M., Barriga, F.J.A.S., 2011. Phosphorus sequestration in Fe-rich sediments from two Brazilian tropical reservoirs. Appl. Geochem. 26, 1607–1622.

Giblin, A.E., Tobias, C.R., Song, B., Weston, N., Banta, G.T., Rivera-Monoroy, V.H., 2013. The importance of dissimilatory nitrate reduction to ammonium (DNRA) in the nitrogen cycle of coastal ecosystem. Oceanography 26 (3), 124–131.

Goldberg, S., 1997. Reactions of boron with soils. Plant Soil 193, 35–48.

Gomis-Yagues, V., Boluda-Botella, N., Ruiz-Bevia, F., 1997. Column displacement experiments to validate hydrogeochemical models of seawater intrusions. J. Contam. Hydrol. 29, 81–91.

Goren, O., Gavrieli, I., Burg, A., Lazar, B., 2011. Cation exchange and $CaCO_3$ dissolution during artificial recharge of effluent to a calcareous sandstone aquifer. J. Hydrol. 400, 165–175.

Holmes, R.M., Aminot, A., Kerouel, R., Hooker, B.A., Peterson, B.J., 1999. A simple and precise method for measuring ammonium in marine and freshwater ecosystems. Can. J. Fish. Aquat. Sci. 56, 1801–1808.

Huang, L.-Y., Li, H.-X., Zhang, X.-M., Lu, W.-S., Liu, Y.-J., 2006. Silicate adsorption in paddy soils of Guangdong, China. Pedoshpere 16, 654–659.

Jones, B.F., Vengosh, A., Rosenthal, E., Yechieli, Y., 1999. Geochemical investigations. In: Bear, J., Cheng, A.H.-D., Sorek, S., Ouazar, D., Herrera, I. (Eds.), Seawater Intrusion in Coastal Aquifers — Concepts, Methods and Practices. Kluwer Academic Publishers, Dordrecht, The Netherlands, pp. 51–71.

Kendall, C., 1998. Tracing nitrogen sources and cycling in catchments. In: Kendall, C., McDonnell, J.J. (Eds.), Isotope Tracers in Catchment Hydrology. Elsevier, pp. 519–576.

Kendall, C., Aravena, R., 2000. Nitrate isotopes in groundwater systems. In: Cook, P., Herczeg, A.L. (Eds.), Environmental Tracers in Subsurface Hydrology. Kluwer Academic Publishers, Dordrecht, The Netherlands, pp. 261–297.

Keren, R., Mezuman, U., 1981. Boron adsorption by clay minerals using a phenomenolgical equation. Clays Clay Miner. 29, 198–204.

Kuenen, J.G., 2008. Anammox bacteria: from discovery to application. Nature 320 (6), 320–326.

Lee, J.S., Ray, R.I., Little, B.J., 2010. Influence of experimental conditions on the outcome of laboratory investigations using natural coastal seawaters. Corrosion 66 (1), 1–6.

Loeppert, R.H., Suarez, D.L., 1996. Carbonate and gypsum. In: Sparks, D.L. (Ed.), Methods of Soil Analysis. Part 3—SSSA Book Series No. 5. ASA and SSSA, Madison, WI, USA, pp. 437–474.

Mariotti, A., Germon, J.C., Hubert, P., Kaiser, P., Letolle, R., Tardieux, A., Tardieux, P., 1981. Experimental determination of nitrogen kinetic isotope fractionation: some principles; illustration for the denitrification and nitrification processes. Plant Soil 62, 413–430.

Mariotti, A., Landreau, A., Simon, B., 1988. ^{15}N isotope biogeochemistry and natural denitrification process in groundwater: application to the chalk aquifer of northern France. Geochim. Cosmochim. Acta 52, 1869–1878.

Mayer, M., Gloss, S.P., 1980. Buffering of silica and phosphate in a turbid river. Limnol. Oceanogr. 25, 12–22.

McIlvin, M.R., Altabet, M.a., 2005. Chemical conversion of nitrate and nitrite to nitrous oxide for nitrogen and oxygen isotopic analysis in freshwater and seawater. Anal. Chem. 77, 5589–5595.

McKeague, J.A., Cline, M.G., 1963. Silica in soil solutions II. The adsorption of monosilicic acid by soil and by other substances. Can. J. Sci. 433, 83–96.

Millero, F., Huang, F., Zhu, X., Liu, X., Zhang, J., 2001. Adsorption and desorption of phosphate on calcite and aragonite in seawater. Aquat. Geochem. 7, 33–56.

Miretzky, P., Conzonno, V., Frenandez Cirelli, Â., 2001. Geochemical processes controlling silica concentrations in groundwaters of the Salado River drainage basin, Argentina. J. Geochem. Explor. 73, 155–166.

Montoya, J.P., Voss, M., 2006. Nitrogen cycling in anoxic waters: Isotopic signatures of nitrogen transformations in the Arabian Sea Oxygen Minimum Zone. In: Neretin, L.N. (Ed.), Past and Present Water Column Anoxia. Springer, Dordrecht, The Netherlands, pp. 257–281.

Obihara, C.H., Russell, E.W., 1972. Specific adsorption of silicate and phosphate by soils. J. Soil Sci. 23 (1), 105–117.

Oliviera, I.B., Demond, A.H., Salezadeh, A., 1996. Packing sands for the production of homogeneous porous media. Soil Sci. Soc. Am. J. 60, 49–53.

Parkhurst, D.L., Appelo, C.A.J., 1999. User's Guide to PHREEQC (version 2): A Computer Program for Speciation, Batch-reaction, One-dimensional Transport, and Inverse Geochemical Calculations. U.S. Geological Survey, Denver, CO, p. 312.

Price, R.M., Savabi, M.R., Jolicoeur, J.L., Roy, S., 2010. Adsorption and desorption of phosphate on limestone in experiments simulating seawater intrusion. Appl. Geochem. 25, 1085–1091.

Rosenfeld, J., 1979. Ammonium adsorption in nearshore anoxic sediments. Limnol. Oceanogr. 24, 356–364.

Russak, A., Sivan, O., 2010. Hydrogeochemical tool to identify salinization or freshening of coastal aquifers determined from combined field work, experiments, and modeling. Environ. Sci. Technol. 44, 4096–4102.

Ruttenberg, K.C., Sulak, D.J., 2011. Sorption and desorption of dissolved organic phosphorus onto iron (oxyhydr)oxides in seawater. Geochim. Cosmochim. Acta 75, 4095–4112.

Rysgaard, S., Thastum, P., Dalsgaard, T., Christensen, P.B., Sloth, N.P., 1999. Effects of salinity on NH_4^+ adsorption capacity, nitrification, and denitrification in Danish estuarine sediments. Estuaries 22, 21–30.

Santoro, A.E., 2010. Microbial nitrogen cycling at the saltwater–freshwater interface. Hydrogeol. J. 18, 187–202.

Seitzinger, S.P., Gardner, W.S., Spratt, A.K., 1991. The effect of salinity on ammonium Sorption in aquatic sediments: Implications for benthic nutrient recycling. Estuaries 14, 167–174.

Siever, R., 1992. The silica cycle in the Precambrian. Geochim. Cosmochim. Acta 56, 3265–3272.

Sigman, D.M., Robinson, R., Knapp, A.N., van Geen, A., McCorkle, D.C., Brandes, J.A., Thunell, R.C., 2003. Distinguishing between water column and sedimentary denitrification in the Santa Barbara Basin using the stable isotopes of nitrate. Geochem. Geophys. Geosyst. 4, 1–20.

Sivan, O., Yechieli, Y., Herut, B., Lazar, B., 2005. Geochemical evolution and timescale of seawater intrusion into the coastal aquifer of Israel. Geochim. Cosmochim. Acta 69, 579–592.

Slomp, C.P., Van Cappellen, P., 2004. Nutrient inputs to the coastal ocean through submarine groundwater discharge: controls and potential impact. J. Hydrol. 295, 64–86.

Sø, H.U., Postma, D., Jakobsen, R., Larsen, F., 2011. Sorption of phosphate onto calcite; results from batch experiments and surface complexation modeling. Geochim. Cosmochim. Acta 75, 2911–2923.

Spiteri, C., Slomp, C.P., Charette, M.a., Tuncay, K., Meile, C., 2008. Flow and nutrient dynamics in a subterranean estuary (Waquoit Bay, MA, USA): field data and reactive transport modeling. Geochim. Cosmochim. Acta 72, 3398–3412.

Stookey, L.L., 1970. Ferrozine–a new spectrophotometric reagent for iron. Anal. Chem. 42, 779–781.

Stumm, W., Morgan, J.J., 1996. Aquatic Chemistry. Wiley, New York.

Stuyfzand, P.J., 1993. Behaviour of major constituents in fresh and salt intrusion waters, in the Western Netherlands. In: Custodio, E. (Ed.), Study and Modeling

of Salt Water Intrusion into Aquifers, Proc. 12th Salt Water Intrusion Meeting. CIHS-CINME, Barcelona, pp. 143–160.
Stuyfzand, P.J., 1998. Quality changes upon injection into anoxic aquifers in the Netherlands: Evaluation of 11 experiments. In: Peters, J. (Ed.), Proceedings of the 3rd International Symposium on the Artificial Recharge of Ground Water, Amsterdam. A.A. Balkema, Rotterdam, pp. 283–291.
Tiessen, H., Moir, J.O., 1993. Total and organic carbon. In: Carter, M.R. (Ed.), Soil Sampling and Methods of Analysis for Canadian Society of Soil Science. Lewis, Boca Raton, FL, pp. 187–199.
Tobias, C.R., Anderson, I.C., Canuel, E.A., Macko, S.A., 2001. Nitrogen cycling through a fringing marsh-aquifer ecotone. Mar. Ecol. Prog. Ser. 210, 25–39.
Ullman, W.J., Chang, B., Miller, D.C., Madson, J.A., 2003. Groundwater mixing, nutrient diagesis, and discharge across sandy beachface, Cap Henlopen, Dalaware (USA). Estuar. Coast. Shelf Sci. 57, 539–552.
Voss, M., Dippner, J.W., Montoya, J.P., 2001. Nitrogen isotope patterns in the oxygen-deficient waters of the Eastern Tropical North Pacific Ocean. Deep-Sea Res. I 48, 1905–1921.
Wood, W.W., Signor, D.C., 1975. Geochemical factors affecting artificial groundwater recharge in the unsaturated zone. Trans. ASAE 18, 677–683.
Yamada, S.S., D'Elia, C.F., 1984. Silicic acid regeneration from estuarine sediment cores. Mar. Ecol. Prog. Ser. 18, 113–118.